Sharp-based, mixed carbonate-siliciclastic shallow-marine deposits (upper Miocene, Betic Cordillera, Spain): the record of ancient transgressive shelf ridges?

Poyatos-Moré M.[1,2], García-García, F.[3], Rodríguez-Tovar F.J.[3], Soria, J.[4], Viseras, C.[3], Pérez-Valera, F.[3] and Midtkandal, I.[2]

1- Departament de Geologia, Universitat Autònoma de Barcelona, Spain.

2- Department of Geosciences, University of Oslo, Norway.

3- Departamento de Estratigrafía y Paleontología, Universidad de Granada, Spain.

4- Departamento de Ciencias de la Tierra y del Medio Ambiente, Universidad de Alicante, Spain.

Corresponding author: miquel.poyatos.geo@gmail.com

Abstract

Isolated sharp-based sedimentary bodies in shelf settings can develop through regressions associated with abrupt lowering of relative sea level, but also via the reworking of regressive deposits during transgressions. An example of these are shelf ridges, observed in modern and ancient shelves, and formed under a wide range of mixed processes. However, despite they have been widely studied partly due to their high reservoir potential, there is still a lack of examples in mixed (carbonate-siliciclastic) successions. This study presents an outcrop example from the Upper Miocene of the Betic Cordillera (Spain), with the aim to propose a depositional and sequence stratigraphic model for the development of transgressive sharp-based mixed deposits, and to provide criteria to differentiate those from their regressive counterparts. The studied succession is ca. 300 m-thick, and shows an alternation of coarse and fine-grained mixed carbonate-siliciclastic deposits. A detailed facies and stratigraphic analysis allows grouping the deposits in several depositional cycles, starting with mudstones (FA1-offshore) or sandy mudstones interbedded with HCS sandstones (FA2-offshore transition), progressively replaced

by coarsening-up, wavy-bedded muddy sandstones (FA3-lower shoreface). These deposits are abruptly truncated by sharp erosive contacts bioturbated by large burrows, passively infilled by overlying coarser bioclastic sediments (FA4-ravinement deposits); burrows are sharp-walled and undeformed, and their ichnological features allow assignation to the *Glossifungites* ichnofacies. These contacts are therefore interpreted as ravinement surfaces. They are overlain by mixed carbonate-siliciclastic units, rich in skeletal fragments and extraclasts, and displaying large-scale sigmoidal cross bedding forming accreting barforms (FA5-mixed bars). The bioclastic sediments overlying the ravinement surfaces combined with these cross-bedded calcarenites form several m-thick and 100's of m-long depositional elements, interpreted as mixed carbonate-clastic shelf ridges. They are capped by thin, highly-cemented and bioturbated sandstones containing maximum flooding surfaces (FA7-condensed deposits). These shelf ridges formed in a shallow-water setting, relatively starved of siliciclastic sediment supply, but with a coeval offshore carbonate factory, which was remobilized and provided skeletal fragments during transgressions. The high amount of extraclasts, organic matter and carbonaceous debris derives from the erosion of older regressive deposits, basement topography or supplied locally via sediment gravity flows. The sharp-based, coarser-grained nature and lithological break at the base of these mixed carbonate-clastic deposits could lead to their misinterpretation as forced-regressive wedges. However, the bioturbated and ravinement nature of their lower contact, combined with the reworked skeletal fragments from an offshore carbonate factory, significantly different from the underlying regressive fine-grained offshore to lower shoreface successions, and the fining, thinning-up stacking of the deposits are consistent with these mixed units forming during transgression. Other studies in relatively time-equivalent deposits have demonstrated the existence of coeval regressive, coarser siliciclastic-dominated shoreline systems in areas relatively close to the studied locality. These studies evidence an actively developing tectonically-driven basin configuration in the area during the upper Miocene, with the development of local depocentres and relatively narrow corridors or seaways in the Mediterranean-Atlantic connection, which could have favoured shelf reworking processes, but also promoted the development of counterintuitive stacking patterns, reflecting the differential interaction between active tectonics and sedimentation across the region.

Keywords: mixed, shelf ridge, transgressive, ravinement, *Glossifungites*, shoreface

Introduction

The origin of sharp-based coarse-grained sedimentary bodies isolated in fine-grained dominated offshore/shelf settings has been a matter of debate for the sedimentary community (see Snedden and Bergman, 1999; Suter and Clifton, 1999). Some studies originally interpreted them as incised valley fills or regressive shallow-marine deposits, transported onto and across the shelf during periods of abrupt lowering of relative sea level (e.g., Plint, 1988; Van Wagoner et al., 1991; Posamentier and Chamberlain, 1993; Bergman and Walker, 1995; 1999; Burton and Walker, 1999; MacEachern et al., 1999). Alternatively, another mechanism for developing and preserving isolated shelf sedimentary bodies involves the reworking of regressive deposits by shelf processes during transgressions. This process can result in the development of shelf ridges, which are relatively large-scale (several m-high, 100s of m-wide, few km long) elongate geomorphic elements observed in a wide range of either tide-, wave- or storm-dominated ancient and modern shelves (e.g., Houbolt 1968; Swift, 1975; Kenyon et al., 1981; Stride et al., 1982; McBride and Moslow 1991; Johnson and Baldwin 1996; van de Meene et al. 1996, Snedden and Dalrymple, 1999; Dyer and Huntley, 1999; Jin and Chough, 2002). Shelf ridge deposits are commonly well sorted, relatively texturally and mineralogically mature, and with extensive and well-preserved overlying and interstratified fine-grained successions, what makes their potential to form good reservoirs high (e.g., Posamentier, 2002; Cattaneo and Steel, 2003; Chiarella et al., 2020).

In the past few years, there has been a renewed interest in shelf ridges, with several studies that have refined previous depositional models (e.g., Snedden et al., 2011; Desjardins et al., 2012; Olariu et al., 2012; Schwarz, 2012; Messina et al., 2014; Leva-López et al., 2016; Michaud and Dalrymple, 2016; Leszczyński and Nemec, 2019; Chiarella et al., 2020). However, most of these studies are from siliciclastic-dominated systems, and so there is still a relative lack of studies of shelf ridges in mixed (carbonate-siliciclastic) successions, with a few exceptions of similar deposits described in ancient straits or seaways (e.g., Longhitano et al., 2012; 2014; Rossi et al., 2017). Besides, in mixed shallow-marine settings, the carbonate factory is not necessarily located close to the coeval shoreline systems supplying the siliciclastic fraction (see Schwarz et al., 2018), which can make the correct identification of isolated shelf sedimentary bodies and their interpretation in terms of sequence stratigraphic concepts more complex.

In this study, an outcrop example from the Upper Miocene of northern Guadix Basin (Spain) is presented, with the aim (i) to characterize and discuss the origin of sharp-based mixed carbonate-siliciclastic deposits in a shallow-marine succession, (ii) to propose a depositional and sequence stratigraphic model for their development in an active tectonic setting, and (iii) to provide criteria to adequately differentiate them from their regressive counterparts

Geological Setting

The Betic Cordillera represents the northern branch of the arcuate Betic-Rif Alpine orogen that closes the westernmost Mediterranean Basin (Alboran Basin) across the Gibraltar Arc (Fig. 1). At the beginning of the Neogene, three major tectono-paleogeographic domains formed and delimited the Betic Cordillera: (1) a fold-and-thrust belt (External Zones or South Iberian Paleomargin), (2) a thrust stack of metamorphic nappe complexes (Internal Zones or Alboran Domain) and (3) allochthonous deposits (Flysch or Gibraltar Units) (Balanyá and García-Dueñas, 1987). The External Zones and the Flysch Units reflect crustal oblique shortening kinematics during the Miocene coeval with crustal extension in the Internal Zones (García-Dueñas et al., 1992; Pérez-Valera et al., 2017). Westward displacement of the Internal Zones configured the two main N-S arcuate thrust systems (Gibraltar and Cazorla Arcs) connected by E-W transfer fault zones (Pérez-Valera et al., 2017). An accretionary complex (Guadalquivir Accretionary Complex) formed by the External Zone Mesozoic to Neogene rocks (including lower to middle Miocene deposits) and it is capped by a gently deformed upper Miocene (Tortonian) Unit. Located close to the Cazorla Arc, this accretionary complex reveals a main stage of tectonic activity during the pre-Messinian Miocene linked to the westward displacement of the Internal Zones (Pérez-Valera et al., 2017).

The study area is located at the central sector of the Betic Cordillera, 20 km to the southwest of the Cazorla arcuate thrust system and very close to a major E-W transfer dextral fault zone (Fig. 1). This study is focused on the lowermost part of a more than 1 km-thick Tortonian marine succession defined by three chronostratigraphic units (from base to top): Unit I, the objective of this study, formed by marine silty marls, sandstones, calcarenites and conglomerates, and defined by *Neogloboquadrina acostaensis* to *humerosa* planktonic foraminifera subzones (Soria, 1993); Unit II, dominated by marine marls interbedded with decimetric-to-metric sandy beds, and defined by *Globorotalia suterae* planktonic foraminifera subzone); and Unit III, represented by coastal cross-stratified mixed siliciclastic-carbonate deposits and large-scale cross-bedded conglomeratic bodies (Soria, 1993; Soria et al., 2003; Reolid et al., 2012). Unit I deposits are also coeval to the oldest marine sediments infilling the neighbouring Guadalquivir foreland basin (Sierro et al., 1996).

Dataset and methods

The succession is displayed in a regional monoclinal structure with strata consistently dipping to the S-SW (Fig. 1). This overall disposition is altered by local syn- and post-depositional faults and changes in direction and dipping of strata which define internal angular unconformities, although these are not necessarily associated to major facies changes. The strata also show an abrupt onlap termination against a highly-tilted algal limestone unit on top of the basement, in this case Mesozoic to Lower Miocene rocks from the External Zone (Soria, 1993), forming the above mentioned accretionary complex (Pérez-Valera et al., 2017) (Fig. 2).

This study is based in the detailed analysis of a 304 m-thick section (Fig. 3), which was measured at cm-scale. Field data were obtained using conventional methodology of logging and describing sedimentary rocks, recording information about lithology (texture and composition), sedimentary structures, ichnological features and composition, bioturbation index (BI of Taylor and Goldring, 1993), orientation of palaeocurrent indicators, scale and geometry of both stratification and sedimentary bodies, and types of contacts. Once measured, the succession was characterized by defining sedimentary facies associations and vertical stratigraphic trends (Figs. 4, 5).

Facies analysis

The succession shows a recurrent alternation of coarse and fine-grained mixed carbonate/siliciclastic deposits (Figs. 3, 5), with dominantly silty marlstones and marly sandstones alternating with m-scale, sharp-based and laterally-continuous mixed siliciclastic-carbonate medium to coarse-grained packages, which are the main objective of this study.

Offshore (FA1)

Whitish grey, massive/structureless to crudely laminated marlstones (Fig. 4A). Subtle grain-size changes occur within mm-scale beds. Bedding contacts are diffuse, but roughly parallel where visible. Bed thicknesses are mm to cm-thick, but packages can reach several meters in thickness (Fig. 5). The fossil content includes planktonic organisms such as foraminifera, sponge spicules and radiolarian (Soria, 1993). Locally large accumulations of well-preserved bivalves, in living position are present, particularly in the lower part of the section (Fig. 5). Bioturbation is absent to low (BI 0-2). These deposits form regionally extensive (several km-long), tabular units, which are used as correlation markers (Fig. 6C). Scattered thin-bedded (up to 10 cm-thick), normally-graded muddy sandstone beds are observed within the mudstone successions, some with erosive bases and rippled tops, and up to moderately bioturbated (BI 0-3).

Interpretation - Distal offshore setting, below storm wave base, with occasional siliciclastic input by low-density turbidity currents and hemipelagic suspension settling.

Offshore transition (FA2)

Grey laminated marlstones, sandy marlstones and sandstone/marlstone heterolithic packages (Fig. 4B). They are interbedded with >10 cm-thick isolated fine to coarse-grained sandstone beds. These beds are tabular or lens shaped, with erosive and/or loaded bases, normal grading and ripple tops, hummocky-cross stratification and common soft-sediment deformation (Fig. 4C, D), and local abundance of organic matter, bioclasts and extraclasts (mainly quartz). Tool marks (mainly flutes) and cross-stratification foresets show paleocurrents ranging to the SW-NW (Fig. 5). These beds can be up to moderately bioturbated (BI 0-3), with vertical or horizontal traces at the top surface (Fig. 7A). Packages range from 8 to 40 m thick (Fig. 5).

Interpretation - Offshore transition setting, above storm-wave base, as evidenced by the common appearance of combined-flow structures in low to high-density turbidity current deposits (Dott and Bourgois, 1982; Duke, 1985; Duke et al., 1991; Dumas et al., 2005). The top of the packages can be gradational to overlying lower shoreface deposits (FA3) or be abruptly truncated by ravinement (FA4) deposits (Fig. 5).

Lower shoreface (FA3)

Grey laminated sandy mudstones to muddy sandstones, with wavy bedding and symmetrical ripple cross-lamination (Fig. 4E, F), and isolated cm-thick beds with low-angle, hummocky and tangential/sigmoidal cross stratification (Fig. 4G) and soft sediment deformation. Paleocurrents from cross-stratified foresets, where observed, point dominantly towards the S-SE. Packages are 3 to 19 m-thick, and tend to stack forming coarsening-up successions (Fig. 5).

Interpretation – Relatively siliciclastic-starved and dominantly low-energy lower shoreface setting, around the fair-weather wave base, as evidenced by the common presence of symmetrical wave ripples, dominant thin bedded and fine-grained nature of the beds, and only occasional appearance of thick sandstone beds with larger-scale combined-flow structures (Yang et al., 2005). They generally display a gradational lower contact from underlying offshore transition deposits (FA2), and are conformably overlain by condensed deposits (FA7) or abruptly truncated by ravinement (FA4) or channel-fill (FA7) deposits (Fig. 5).

Ravinement deposits (FA4)

Yellow medium to very coarse-grained, structureless bioclastic calcarenites (Fig. 4H). Beds are 60 to 250 cm-thick and moderately to highly bioturbated (BI 3-5) (Fig. 5). They have a sharp, erosive highly bioturbated base, with vertical, sub-vertical and oblique J-shaped burrows and shallow cylindrical rounded structures, as well as circular sections and horizontal, branched, forms. Most traces can be assigned to *Thalassinoides*, but with local presence of *Rhizocorallium*, *Skolithos* and *Bergaueria*. Burrows are undeformed and characterized by sharp contacts, showing, in some cases a penetration depth up to around 20 cm into the underlying deposits, and are passively infilled by mixed carbonate-clastic sediment (Fig. 7B, C). This includes abundant skeletal fragments (bivalves, bryozoans, red algae, echinoids), organic matter, carbonaceous debris and extraclasts (quartz and volcanic-rock fragments), in a relatively poorly-sorted organization. Normally-graded tops occur.

Interpretation – The ichnological features found at the base of these deposits allow assignation to the *Glossifungites* ichnofacies, developed into compacted, semi-lithified substrates (Seilacher, 1967). The contacts are therefore interpreted as transgressive ravinement surfaces (MacEachern et al., 1992; Bann et al., 2004; Rodríguez-Tovar et al., 2007), although evidence are not conclusive to associate them to any particular dominant process regime (e.g. waves or tides). The poorly-sorted and bioclastic-rich beds immediately overlying these surfaces are consequently interpreted as ravinement deposits (Zecchin et al., 2019), resulting from the remobilization of a coeval offshore/alongshore carbonate factory, mixed with the erosion of underlying offshore transition (FA2) and lower shoreface (FA3) deposits. However, the reworking of forced-regressive poorly-sorted sandstone wedges as well as the entrainment of immature extraclasts from intrabasinal basement highs cannot be ruled out. They are commonly found abruptly truncating offshore transition (FA2) or lower shoreface (FA3) deposits, and overlain my mixed bar (FA5) or condensed (FA6) deposits.

Mixed bars (FA5)

Yellow fine to coarse-grained, cross-bedded bioclastic calcarenites (Fig. 4I, J). Beds are moderately to highly bioturbated (BI 3-5; Fig. 7D, E, F), with traces including dominant *Planolites,* well-developed *Thalassinoides* structures, vertical *Ophiomorpha* shafts, and local *Bichordites/Scolicia* (Fig. 6D, E, F). Loaded bases are common, and arranged in stacked single or multiple sets of large-scale sigmoidal cross-bedding (up to 6 m-thick, Figs. 5, 6), with abundant skeletal fragments (dominantly bivalves, but also bryozoans, red algae, echinoids), organic matter, carbonaceous debris and extraclasts (quartz and volcanic-rock fragments) (Fig. 4K), and a relatively sharp top, occasionally highly cemented and concretionary. Bars show bidirectional accretion directions ranging towards the S and N, although southward accretion dominates (Fig. 5).

Interpretation - They are interpreted as mixed siliclastic-carbonate barforms, resulting from the reworking of transgressive ravinement deposits (FA4), possibly accumulated preferentially in some areas of the seabed, favouring or promoting their reworking by shelf currents.

Condensed section (FA6)

Grey-yellow, intensely bioturbated sandstones (BI 5-6; Fig. 7G), with bioclasts (mainly bivalve fragments) and often highly cemented or forming concretionary horizons (Fig. 4N, O). Traces include *Scolicia* showing cross-cutting relationships in the bed top surfaces (Fig. 7G). Beds are generally thin (up to 20 cm), but packages reach up to 1.5 m.

Interpretation - Their high bioturbation index and concretionary/cemented nature are consistent with condensed deposits, formed under low energy, low sedimentation rate conditions, associated with regional flooding events. They are often found conformably overlying lower shoreface deposits (FA3) or mixed bars (FA5), and overlain by offshore (FA1) or offshore transition (FA2) fine-grained deposits (Fig. 5).

Channel-fill (FA7)

Bioclastic, cross-bedded pebbly sandstones, stacked in an up to 5 m-thick package, with a concave-up erosive base (Fig. 4L). The package is slightly fining-up, and contains a mix of skeletal fragments (dominantly bivalves, but also bryozoans and red algae), organic matter and large (up to several cm-long) angular extraclasts (quartz and volcanic fragments), more concentrated towards the base (Fig. 4M, 4). This facies association has only been recognized in the upper part of the studied section (Fig. 5).

Interpretation - These deposits are interpreted as subaqueous channel/gulley fills, possibly containing a regressive surface of marine erosion at the base, consistent with the large presence of landward material, mixed with transgressive ravinement deposits (FA4), and overlain by mixed bars (FA5) (Fig. 5). They might be the only preserved expression of forced-regressive deposits.

Stratigraphy

This section describes the studied succession summarized in Fig. 5. It starts with 28 m of dominantly structureless to faintly laminated mudstones, with subordinate cm-thick sandstone beds, some with erosive bases and rippled tops (FA1 – offshore, Table 1, Fig. 4A), with paleocurrents pointing towards the W-NW and up to moderately bioturbated (BI 0-3). The mudstones contain a significant amount of bivalves in living position. After this, the following 14 m show an alternation of mudstones and sandstone/mudstone heterolithic packages, with wavy lamination and combined-flow ripples (FA2 – offshore transition, Table 1, Fig. 4C, D). The next 3 m show a coarsening-up package of sandy mudstone to muddy sandstone, with wavy bedding towards the top (FA3 – lower shoreface, Table 1, Fig. 4E), and culminating with a 20 cm-thick, intensely bioturbated sandstone (BI 5-6) (FA6 – condensed deposits, Table 1, Fig. 4N).

The next 21 m contain laminated mudstones with >10 cm-thick isolated sandstone beds, with hummocky-cross stratification and common soft-sediment deformation, and several m-thick sandstone/mudstone heterolithic packages, with cm-thick combined-flow ripple-laminated beds and hummocky cross-stratification (FA2 – offshore transition), with paleocurrents pointing towards W-SW. These beds can be up to moderately bioturbated (BI 0-3), with vertical or horizontal traces at the top surface (Fig. 7A). The top of the package is gradational to the following 11 m, which show a slightly coarsening-up succession of sandy mudstone to muddy sandstone, with wavy bedding, symmetrical ripple cross-lamination, interbedded with isolated cm-thick beds with hummocky-cross stratification and soft sediment deformation (FA3 – lower shoreface). Paleocurrents point towards W-NW (Fig. 5). This succession culminates with a 1.5 m-thick, intensely bioturbated sandstone (BI 5-6), with a highly cemented top (FA6 – condensed deposits).

The next 8.75 m are composed of structureless to laminated mudstones interbedded with >10 cm-thick isolated sandstone beds, with hummocky-cross stratification, and common soft-sediment deformation (FA2 – offshore transition). The following 12 m show a muddy sandstone succession, slightly coarsening-up at the base, with wavy bedding and symmetrical ripple cross-lamination, and with a few cm-thick sandstone beds (FA3 – lower shoreface). This succession is abruptly truncated by a 60 cm-thick, bioclastic calcarenite, with a highly bioturbated base (FA4 – ravinement deposits, Table 1, Fig. 4H). This is overlain by a 40 cm-thick muddy sandstone package, which is also abruptly truncated by a 1 m-thick, highly bioturbated, highly bioclastic calcarenite, with abundant bivalve fragments, and finally by a 1 m-thick, amalgamated pebbly sandstone package (FA5 – mixed bars, Table 1), with a highly cemented, concretionary top.

The next ca. 8 m contain dominantly structureless mudstones, with subordinate cm-thick sandstone/mudstone heterolithic packages (FA1 – offshore), overlain by a 38 m-thick succession of structureless sandy mudstones, with a few >20 cm-thick medium to coarse-grained sandstone beds (FA2 – offshore transition). These beds show erosive bases, normal grading and current ripple tops, and local abundance of organic matter and extraclasts (mainly quartz and volcanic rock fragments). Paleocurrent indicators point towards the W (Fig. 5). This succession is abruptly overlain by a 180 cm-thick, coarse-grained bioclastic calcarenite with a highly bioturbated base (FA4 – ravinement deposits), and abundant skeletal fragments (bivalves, bryozoans, red algae), organic matter and extraclasts (mainly quartz fragments). The overlying 4 m are composed of moderately to highly bioturbated (BI 3-5), bioclastic calcarenites, with large-scale cross-bedding (migrating towards the S, Fig. 5), skeletal fragments and extraclasts (FA5 – mixed bars, Fig. 4I, J, K), and a relatively sharp top.

The next 23 m show a succession of structureless to faintly laminated sandy mudstones, with a few >10 cm-thick fine to coarse-grained sandstone beds (FA2 – offshore transition). The beds are tabular or lens shaped, and show erosive and/or loaded bases, normal grading and combined-flow ripple tops, and local abundance of bioclasts and extraclasts (mainly quartz). This succession is abruptly truncated by a 2.5 m-thick, bioclastic calcarenite, with a highly bioturbated base (FA4 – ravinement deposits). The calcarenite shows normal grading, with abundance of skeletal (bivalves, bryozoans, red algae), organic matter fragments and carbonaceous debris, and it is in turn abruptly overlain by another 1.5 m-thick, sharp-based, highly bioturbated calcarenite, with abundant bivalve fragments and extraclasts (mainly quartz and volcanic rock fragments). The overlying 3.8 m are composed of highly bioturbated (BI 4-5) bioclastic calcarenites, with loaded bases, large-scale sigmoidal cross-bedding (migrating towards the S, Fig. 5), and skeletal fragments (mainly bivalves) (FA5 – mixed bars). After these, there are 60 cm of a muddy sandstone, overlain by a highly-cemented, bioclastic (mainly bivalve fragments) and a highly bioturbated (BI 5-6) calcarenite (FA7 – condensed section).

The following 24 m are a succession of structureless to laminated sandy mudstones, interbedded with sandstone/mudstone heterolithic packages and >10 cm-thick sandstone beds, with wavy lamination, combined-flow ripples and low-angle cross-stratification (FA2 – offshore transition), with paleocurrents pointing towards the N and S (Fig. 5). These deposits are abruptly truncated by a 180 cm-thick, bioclastic calcarenite, with a sharp, highly bioturbated base (FA4 – ravinement deposits). The calcarenite shows abundant skeletal fragments (bivalves, bryozoans, red algae), organic matter and extraclasts (mainly quartz and volcanic fragments). The overlying 1 m are a muddy sandstone, abruptly truncated by a 5.5 m of moderately to highly bioturbated (BI 3-5) bioclastic calcarenites, with large-scale sigmoidal cross-bedding, skeletal fragments (mainly bivalves), organic matter and carbonaceous debris (FA5 – mixed bars). The package shows several stacked sets of accreting barforms (Fig. 6B), with sets oriented towards the S and N (Fig. 5), and a relatively sharp contact with the overlying deposits.

The following 31 m are a succession of structureless to laminated sandy mudstones, interbedded with sandstone/mudstone heterolithic packages and >10 cm-thick sandstone beds, with erosive and/or loaded bases, wavy lamination and combined-flow ripples (FA2 – offshore transition). The mudstones contain local accumulations of bivalves in living position. The upper part of this succession is gradational to the following 4 m, which show a slightly coarsening-up succession of sandy mudstone to muddy sandstone, with wavy bedding, symmetrical ripple cross-lamination, with an isolated 80 cm-thick sandstone bed with pervasive soft sediment deformation (FA3 – lower shoreface). These deposits are abruptly truncated by a 5 m-thick bioclastic, cross-bedded pebbly sandstone package, with a concave-up erosive base (FA6 – channel fill, Table 1, Fig. 4L, M). The package is slightly fining-up, and contains a mix of skeletal fragments (dominantly bivalves, but also bryozoans and red algae), organic matter and large (up to several cm-long) angular extraclasts (quartz and volcanic fragments), more concentrated towards the base. The package is overlain by a 80 cm-thick muddy sandstone, which truncated by 6 m-thick, thinning-up package of calcarenites and muddy calcarenites, with several beds displaying large-scale low angle cross bedding (oriented towards the S, Fig. 5), and abundance of bioclasts and suboardinate extraclats (mainly quartz) (FA5 – mixed bars). These deposits show a relatively sharp transition into the overlying 70 cm-thick sandy mudstone, overlain by a 1.5 m-thick highly bioturbated (BI 5-6) calcarenitic package (FA7 – condensed section, Fig. 4O).

The following 16 m are a succession of structureless to faintly laminated mudstones, interbedded with several cm-thick sandstone beds, with wavy lamination and hummocky cross-stratification (FA2 – offshore transition). Sandstone beds are up to moderately bioturbated (BI 0-3). This succession grades into the following 19 m, which show a coarsening-up package of sandy mudstone to muddy sandstone, with wavy bedding and symmetrical ripple cross-lamination (FA3 – lower shoreface, Fig. 4F). This package is abruptly truncated by a 1.8 m-thick, bioclastic calcarenitic package, with a sharp, highly bioturbated base, and low-angle sigmoidal cross-bedding (FA5 – mixed bars), overlain by 60 cm of muddy sandstones and 20 cm of a highly bioturbated (BI-5-6) sandstone (FA7 – condensed section).

Stratigraphic cyclic arrangement

The succession is composed of at least 8 cycles (C1-C8), each of them 23 to 45 m-thick (Figs. 4, 5). Cycles start with offshore mudstones (FA1) or offshore transition deposits (FA2). In some cycles (Cycles 1-3 and 7-8, Fig. 5), these are progressively replaced by lower shoreface deposits

(FA3). In the upper cycles (Cycles 3-8, Fig. 5), offshore transition or lower shoreface deposits are abruptly truncated by erosive contacts bioturbated by large, sharp-walled burrows, passively infilled by overlying mixed carbonate-clastic sediments, which in places penetrate a few cm into the strata below (Fig. 7B, C). They are overlain by poorly- to moderately-sorted mixed carbonate-clastic units, rich in skeletal fragments and extraclasts (mainly quartz and volcanic fragments), and often displaying large-scale sigmoidal cross bedding, interpreted as ravinement deposits (FA4) and mixed bars (FA5). These deposits are moderately to highly bioturbated (BI 3-5), and capped by marls interbedded with highly-cemented and bioturbated sandstones, with high ichnodiversity, and interpreted as condensed sections containing condensed maximum flooding surfaces (FA7).

Discussion

A siliciclastic-starved shelf and the origin of the remobilized carbonate factory

The studied succession is interpreted to have deposited in a relatively shallow-water shelf (Fig. 8A), dominantly above storm-wave base, as suggested by the evidence of storm-reworking in the gravity flow deposits within the more distal, finer-grained packages. The partial preservation and fine-grained nature of the coarsening and thickening up successions of offshore transition (FA2) to lower shoreface (FA3) deposits suggests there was a coeval north-westward prograding shoreline system, although the shelf was relatively starved in terms of coarse-grained siliciclastic sediment supply, due to either a) a distal position with respect to the delivery systems, or b) a period of relative low influx of siliciclastic sediment. However, offshore transition deposits are abruptly truncated by mixed clastic-carbonate units, through sharp, highly bioturbated transgressive ravinement surfaces (MacEachern et al., 1992; Bann et al., 2004). The overlying deposits, including coarse-grained, skeletal-rich bioclastic calcarenites (FA4) and large-scale sigmoidal cross-bedded calcarenites displaying single to multiple accreting barforms (FA5) formed transgressive mixed carbonate-clastic shelf ridges. These deposits contain dominantly skeletal fragments, mainly from bivalves, but also from bryozoans, red algae and echinoids, suggesting the nearby presence of a coeval carbonate factory. Because those skeletal fragments are only contained in the transgressive mixed clastic-carbonate units, this implies the carbonate factory was located in either i) a more distal position within the shelf, or ii) a lateral position within the shelf. A scenario where the carbonate factory is not necessarily located close to the equivalent shoreline supplying the siliciclastic fraction can occur quite commonly in mixed carbonate-siliciclastic shallow-marine systems (Schwarz et al., 2018). Also, a similar arrangement has been reported in time-equivalent deposits close to the study area (Tabernas Basin, see Fig. 1b), where a high-frequency cyclicity is represented by shallow-water (15-20 m-deep) calcarenites (with bryozoans and red algae skeletal fragments) overlying coastal systems (Gilbert-type wave-dominated deltas) during transgressive pulses (García-García et al., 2006b). Several of the mixed units in the studied section are poorly sorted and also contain a relatively high amount of extraclasts (mainly quartz and volcanic fragments), organic matter and carbonaceous debris. This contrasts with conventional transgressive shelf ridges, mostly composed of well-sorted sandstones (Cattaneo and Steel, 2003), particularly those undergoing long-term reworking/remoulding during their migration across the shelf (Snedden and Dalrymple 1999). The coarse and angular nature of some of them suggest they might derive from i) short-term, high-energy storm-reworking of older forced-regression poorly-sorted sandstone wedges, ii) local erosion of underlying basement topography or iii) reworked sediment gravity flow deposits, as extraclasts and organic debris are also observed in normally-graded turbidite beds within offshore transition deposits.

Depositional model for the development of transgressive mixed carbonate-clastic shelf ridges

An evolutionary model for the development and preservation of sharp-based, mixed carbonate-clastic transgressive shelf ridges is proposed and summarised in Fig. 9. During regressive periods, the limited north-westward normal progradation of a relatively distal shoreline resulted in a dominantly siliciclastic-starved shelf, formed by coarsening-up successions of marlstone-dominated offshore (FA1) to offshore transition (FA2) deposits, and local preservation of lower shoreface muddy sandstone deposits (FA3) (Fig. 9A). This shelf, dominated by fine-grained carbonate deposits, was only receiving siliciclastic sediment (including extraclasts and organic debris) occasionally via forced regressions and/or gravity flows (e.g. hyperpycnal flows), which underwent storm reworking during or shortly after deposition, and resulted in discrete cm-thick sandstone beds within offshore transition deposits (Fig. 9B) (Myrow et al., 2002; Pattison et al., 2007; Lamb et al., 2008; Jelby et al., 2019). After some time (enough to compact and lithify the substrate), offshore transition to lower shoreface deposits were partially removed during transgression, with the development of an erosive and highly bioturbated contact, interpreted as a transgressive ravinement surface (Fig. 9C), due to the undeformed and sharp nature of the burrows (Fig. 7B, C) and their association to *Glossifungites* ichnofacies. This ravinement surface was followed by deposition of a relatively poorly-sorted assemblage of mixed deposits (FA4), dominated by skeletal fragments resulting from the remobilization of a more distal offshore or alongshore carbonate factory (Fig. 9D). The uneven accumulation of these mixed deposits on the seabed possibly resulted in areas that favoured higher reworking via shelf (most likely storm-wave) processes and nucleation of laterally extensive shelf ridges, with the development of sigmoidal cross-bedded barforms (FA5) (Fig. 9E). These can locally show bidirectional accretion orientations (N-S), but dominantly pointing southward, at a high angle with respect to the dominantly westward orientation of unidirectional paleocurrents recorded from gravity flow deposits (Fig. 8B). Continued transgression resulted in regional flooding, increased water depth and decrease of reworking processes and deposition, leading to lower sedimentation rates and the development of highly biortubated, condensed deposits (FA7), containing a maximum flooding surface, and locally preserved above the shelf ridges (Fig. 9F). Finally, the renewed advancement of the regressive shoreline system led to progressive higher deposition of fine-grained sediments in offshore and offshore-transition settings, resulting in the burial and effective preservation of the underlying mixed carbonate-clastic shelf ridges (Fig. 9G). The tectonically active setting possibly contributed further to the preservation of such a thick succession.

Shoreface-connected versus offshore sand ridges

Many inner continental shelves present large bedforms evolving from proximal (coastal) areas represented by shoreface-connected ridges to distal (offshore) areas represented by shelf sand ridges (e.g. Schwab et al., 2013). Shoreface-connected ridges show shore-oblique crest direction and more parallel offshore ridges (also called shoreface-detached ridges or ‘drowned’ ridges, Snedden et al., 2011) (Nnafie et al., 2015). Shoreface-connected ridges are commonly linked to storm-dominated coasts to shelves in depths of 10-20 m where feedbacks occur between storm-driven longshore currents and the sandy seabed (Trowbridge, 1995). The absence of an efficient segregation of heterolithic grains in the studied mixed shelf ridges is consistent with high-energy conditions induced by a persistent storm-wave action, which is more characteristic at the shoreface zone than at offshore-transition settings where tidally-modulated segregation commonly occurs (Chiarella et al., 2012). The textural nature of (mainly) the lower to middle parts of studied shelf ridges (more poorly-sorted and coarser-grained than conventional tidal-dominated offshore ridges) are consistent with their initial development closer to coastal zones where sediment reworking by storm waves (or tidal currents) and sediment supply by rivers are common processes (van Heteren et al., 2011; Rossi et al., 2017). In fact, coeval interplay of shallow-water carbonate factories and coarse-grained delta development is reported along the same tectonically-active margin close to the study area (García-García et al., 2006b). Additionally, well-developed burrowed ravinement basal surfaces and relatively short ridges (with single cross-bedding sets, and not forming compound bars) are more characteristic of gentle slopes (Nnafie et al., 2014) and shallower-water settings (i.e. shoreface). Simulations of sand ridges with morphodynamic models conclude that the morphology and activity of sand ridges are controlled by the rate of sea level rise, depth and coastal-shelf slope (Nnafie et al., 2014). Following those models, the shelf ridges studied here, with more common examples of single than compound barforms, would have been enhanced during low rates of sea level rise on gentle coastal to inner shelf slopes.

Implications for equivalent or other similar successions

The sharp-based, coarser-grained nature and significant lithological break at the base of these shallow-marine deposits has been proposed in other studies as criteria for detached forced-regressive wedges (e.g. Hunt and Tucker, 1992; Ainsworth et al., 2000; Fitzsimmons and Johnson, 2000; Posamentier and Morris 2000; García-García et al., 2011). However, the bioturbated ravinement bases of the studied bodies, the presence of skeletal fragments from an offshore carbonate factory, significantly different from the underlying offshore transition to lower shoreface deposits, and the fining, thinning-up stacking of the deposits are consistent with these mixed units being interpreted as transgressive deposits (Fig. 8C). Other studies in relatively time-equivalent deposits in the southern margin of the Guadix Basin and in the northern margin of the Guadalquivir Foreland Basin have demonstrated the existence of coeval regressive, siliciclastic-dominated shoreline systems (García-García et al., 2014; 2021), in areas relatively close to the studied locality. These studies evidence the existence of a complex and dynamic basin configuration in the upper Tortonian, with the development of local depocentres and relatively narrow corridors or seaways during the connection between the Mediterranean and Atlantic (Betzler et al., 2006; Martín et al., 2014). This configuration possibly triggered intensification of bottom currents and favoured shelf reworking processes such as tidal amplification, as also seen in overlying deposits (García-García et al., 2009), and in the nearby Rifian corridor (Capella et al., 2017; de Weger et al., 2020; Beelen et al., 2021; Miguez-Salas et al., 2021) but also promoted the development of local sediment entry points and counterintuitive stacking patterns, which reflect the differential interaction between active tectonics and sedimentation across the region (e.g. Ándric et al., 2018).

Conclusions

This study analyses and discusses the origin and development of sharp-based, mixed carbonate-siliciclastic deposits in a shallow-marine succession from the Upper Miocene of the Betic Cordillera (Spain). The studied succession (ca. 300 m-thick) shows a recurrent alternation of coarse and fine-grained mixed carbonate-siliciclastic deposits, arranged in 8 depositional cycles, starting with mud-prone offshore/offshore transition deposits, progressively replaced by sand-prone lower shoreface deposits. These are abruptly truncated by sharp, highly bioturbated contacts (*Glossifungites* ichnofacies), passively infilled by poorly-sorted, coarser bioclastic deposits and interpreted as ravinement surfaces. They are overlain by mixed carbonate-siliciclastic sigmoidal barforms, rich in skeletal fragments and extraclasts, forming several m-thick and 100's of m-long depositional elements, interpreted as mixed carbonate-clastic shelf ridges, and capped by condensed deposits containing maximum flooding surfaces. These ridges formed in a shelf which received occasional siliciclastic supply via sediment gravity flows, but with a coeval offshore carbonate factory, eroded and remobilized during transgressions. These sharp-based mixed carbonate-clastic deposits could be tentatively misinterpreted as forced-regressive wedges in other studies. However, this work provides criteria to distinguish them, including the nature of their lower contact, presence of reworked skeletal fragments and their stacking pattern, which are consistent with their interpretation as transgressive deposits. When put in context with other studies in relatively time-equivalent regressive and more siliciclastic-dominated successions nearby, this evidences a complex configuration of the Mediterranean-Atlantic connection during the upper Miocene, with sea corridors increasing currents and shelf reworking processes, and local sediment supplies and depocentres resulting in laterally variable stacking patterns, and reflecting differential and complex tectono-sedimentary interactions.

Acknowledgements

This work was supported by Aker BP (ShelfSed project, University of Oslo) and Agencia Estatal de Investigación (AEI) y Fondo Europeo de Desarrollo Regional (FEDER) (CGL2017-89618-R project, University of Granada). The study by RT was funded by the project PID2019-104625RB-100 (Secretaría de Estado de I + D + I, Spain), Research Group RNM-178 (Junta de Andalucía), B-RNM-072-UGR18 (FEDER Andalucía), and P18-RT-4074 (Junta de Andalucía), and the Scientific Excellence Unit UCE-2016-05 (Universidad de Granada).

References

Ainsworth, R.B., Bosscher, H., Newall, M.J., 2000. Forward stratigraphic modelling of forced regressions: evidence for the genesis of attached and detached lowstandsystems. In: Hunt, D., Gawthorpe, R.L. (Eds.), Sedimentary Response to Forced Regressions: Geol. Soc. London, Spec. Publ., vol. 172, 163–176.

Balanyá, J. C., García-Dueñas, V., 1987. Les directions structurales dans le Domaine d'Alboran de part et d'outre du Detroit de Gibraltar, C. R. Acad. Sci., Ser. II, 304, 929–933.

Bann, K.L., Fielding, C.R., MacEachern, J.A., Tye, S.C., 2004. Differentiation of estuarine and offshore marine deposits using integrated ichnology and sedimentology: Permian Pebbley Beach Formation, Sydney Basin, Australia. In: McIlroy, D. (Ed.), The application of ichnology to palaeoenvironmental and stratigraphic analysis. Geological Society, Special Publications, vol. 228, pp. 179–211. London.

Beelen, D., Wood, L., Najib Zaghloul, M., Haissen, F., Arts, M., Ouahbi, I., Redouane, M., Cardona, S., 2020. Tide-dominated deltas responding to high-frequency sea-level changes, pre-Messinian Rifian Corridor, Morocco. Journal of Sedimentary Research, 90, 1642-1666.

Bergman, K.M., Walker, R.G., 1995. High-resolution sequence stratigraphic analysis of the Shannon sandstone in Wyoming, using a template for regional correlation. Journal of Sedimentary Research, 2, 255-264.

Bergman, K., Walker, R.G., 1999. Campanian Shannon sandstone: an example of a falling stage systems tract deposit. In: Isolated Shallow Marine Sand Bodies: Sequence stratigraphic analysis and sedimentologic interpretation (Bergman, K.M., Snedden, J.W., Eds.). SEPM Spec. Pub., 64, 85-93.

Burton, J., Walker, R.G., 1999. Linear transgressive shoreface sandbodies controlled by fluctuations of relative sea level: Lower Cretaceous Viking Formation in the Joffre-Mikwan-Fenn area, Alberta, Canada. In: Isolated Shallow Marine Sand Bodies: Sequence stratigraphic analysis and sedimentologic interpretation (Bergman, K.M., Snedden, J.W., Eds.). SEPM Spec. Pub., 64, 255-272.

Cattaneo, A., Steel R.J., 2003. Transgressive deposits: a review of their variability. Earth-Science Reviews, 62, 187-228.

Chiarella, D., Longhitano, S.G., Sabato, L., Tropeano, M., 2012. Sedimentology and hydrodynamics of mixed (siliciclastic-bioclastic) shallow-marine deposits of Acerenza (Pliocene, Southern Apennines, Italy). Ital. J. Geosci., 131 (1), 136-151.

Chiarella, D., Longhitano, S.G., Mosdell, W., Telesca, D., 2020. Sedimentology and facies analysis of ancient sand ridges: Jurassic Rogn Formation, Trondelag Platform, offshore Norway. Marine and Petroleum Geology, 112, 1-16.

Desjardins, P.R., Buatois, L.A., Mangano, M.G., 2012. Tidal flats and subtidal sand bodies. In: Trace fossils as indicators of sedimentary environments (Knaust, D., Bromley, R.G., eds.). Developments in Sedimentology, 64, 529-561.

Do Couto, D., Gumiaux, C., Augier, R., Lebret, N., Folcher, N., Jouannic, G., Jolivet, L., Suc, J.P., Gorini, C., 2014. Tectonic inversion of an asymmetric graben: Insights from a combined field and gravity survey in the Sorbas basin. Tectonics, 33, 1360-1385.

Dott, R.H., Bourgois, J., 1982. Hummocky stratification: significance of its variable bedding sequences. Geological Society of American Bulletin 93, 663–668.

Duke, W.L., 1985. Hummocky cross-stratification, tropical hurricanes, and intense winter storms. Sedimentology 32, 167–194.

Duke, W.L., Arnott, R.W.C., Cheel, R.J., 1991. Shelf sandstones and hummocky cross-stratification: new insights on a stormy debate. Geology 19, 625–628.

Dumas, S., Arnott, R.W.C., Southard, J.B., 2005. Experiments on oscillatory-flow and combined-flow bed forms: implications for interpreting parts of the shallow-marine sedimentary record. Journal of Sedimentary Research 75 (3), 501–513.

Dyer, K.R., Huntley, D.A., 1999. The origin, classification and modelling of sand banks and ridges. Continental Shelf Research, 19, 1285-1330.

Fitzsimmons, R., Johnson, S., 2000. Forced regressions: recognition, architecture and genesis in the Campanian of the Bighorn Basin, Wyoming. In: Hunt, D., Gawthorpe, R.L. (Eds.), Sedimentary Response to Forced Regressions: Geol. Soc. London, Spec. Publ., vol. 172, pp. 113–140.

García-Dueñas, V., Balanyá, J.C., Martínez-Martínez, J.M., 1992. Miocene extensional detachments in the outcropping basement of the northern Alborán Basin (Betics) and their tectonic implications, Geo. Mar. Lett., 12, 88–95.

García-García, F., Fernández, J., Viseras, C., Soria, J.M., 2006a. Architecture and sedimentary facies evolution in a delta stack controlled by fault growth (Betic Cordillera, southern Spain, late Tortonian). Sedimentary Geology, 185, 79-92.

García-García, F., Fernández, J., Viseras, C., Soria, J.M., 2006b. High frequency cyclicity in a vertical alternation of Gilbert-type deltas and carbonate bioconstructions in the late Tortonian, Tabernas Basin, Southern Spain. Sedimentary Geology, 192, 123-139.

García-García, F., Soria, J., Viseras, C. Fernández, J., 2009. High-frequency rhythmicity in a mixed siliciclastic-carbonate shelf (Late Miocene, Guadix Basin, Spain): A model of interplay between climatic oscillations, subsidence and sediment dispersal. Journal of Sedimentary Research, 79, 302-315.

García-García, F., De Gea, G.A., Ruiz-Ortiz, P.A., 2011. Detached forced-regressive shoreface wedges at the Southern Iberian continental palaeomargin (Early Cretaceous, Betic Cordillera, S Spain). Sedimentary Geology, 236, 197-210.

García-García, F., Rodríguez-Tovar, F.J., Poyatos-Moré, M., Yeste, L.M., Viseras, C., 2021. Sedimentological and ichnological signatures of an offshore-transitional hyperpycnal system (Upper Miocene, Betic Cordillera, southern Spain). Palaeogeography, Palaeoclimatology, Palaeoecology, 561, 1-11.

Houbolt, J.J.H.C., 1968. Recent sediments in the Southern Bight of the North Sea. Geol. Mijnbouw, 47, 245-273.

Hüsing, S.K., Oms, O., Agustí, J., Garcés, M., Kouwenhoven, T.J., Krijgsman, W., Zachariasse, W.-J., 2010. On the late Miocene closure of the Mediterranean- Atlantic gateway through the Guadix basin (southern Spain). Palaeogeography Palaeoclimatology Palaeoecology 291, 167–179.

Jin, J.H., Chough, S.K., 2002. Erosional shelf ridges in the mid-eastern Yellow Sea. Geo-Mar Lett, 21, 219-225

Johnson, H.D., Baldwin, C.T., 1996. Shallow clastic seas. In: Sedimentary environments: processes, facies and stratigraphy (Reading, H.G., ed.). 3rd edition, 232-280.

Kenyon, N.H., Belderon, R.H., Stride, A.H., Johnson, M.A., 1981. Offshore tidal sand-banks as indicators of net sand transport and as potential deposits. In: Holocene marine sedimentation in the North Sea Basin (Nio, S.D., Shüttenhelm, R.T.E., Van Weering, Tj.C.E., eds). IAS Spec. Pub., 5, 257-268.

Leszczynski, S., Nemec, W., 2019. Sedimentation in a synclinal shallow-marine embayment: Coniacian of the North Sudetic Synclinorium, SW Poland. Depositional Rec., 6, 144-171.

Leva-López, J., Rossi, V.M., Olariu, C., Steel, R.J., 2016. Architecture and recognition criteria of ancient shelf ridges; an example from Campanian Almond Formation in Hanna Basin, USA. Sedimentology, 63, 1651-1676.

Longhitano, S.G., Mellere, D., Steel, R.J. Ainsworth, R.B., 2012. Tidal Depositional systems in the Rock Record: a Review and New Insights. In: Modern and Ancient Depositional Systems: Perspectives, Models and Signatures (Eds S.G. Longhitano, D. Mellere and R.B. Ainsworth), Sed. Geol. Spec. Issue, 279, 2–22.

Longhitano, S.G., Chiarella, D., Muto, F., 2014. Three-dimensional to two-dimensional cross-trata transition in the lower Pleistocene Catanzaro tidal strait transgressive succession (southern Italy). Sedimentology, 61, 2136-2171.

MacEachern, J.A., Raychaudhuri, I., Pemberton, S.G., 1992. Stratigraphic applications of the Glossifungites ichnofacies: delineating discontinuities in the rock record. In: Pemberton, S.G. (Ed.), Applications of Ichnology to Petroleum Exploration: A Core Workshop. Core Workshop, vol. 17. Society of Economic Paleontologists and Mineralogists, Tulsa, OK, pp. 169–198.

MacEachern, J.A., Zaitlin, B.A., Pemberton, S.G., 1999. A sharp-based sandstone of the Viking Formation, Joffre Field, Alberta, Canada: Criteria for recognition of transgressively incised shoreface complexes. Journal of Sedimentary Research, 69 (4), 876-892.

Messina, C., Nemec, W., Martinius, A.W., Elfenbein, C., 2014. The Garn Formation (Bajocian-Bathonian) in the Kristin Field, Halten Terrace: its origin, facies architecture and primary heterogeneity model. Int. Assoc. Sedimentol. Spec. Publ., 46, 513-550.

Michaud, K.J., Dalrymple, R.W., 2016. Facies, architecture and stratigraphic ocurrence of headland-attached tidal sand ridges in the Roda Formation, Northern Spain. In: Contributions to modern and ancient tidal sedimentology: Proceeding of the Tidalites 2012 conference (Tessier B., Reynaud, J.Y., eds.). Int. Assoc. Sedimentol. Spec. Publ., 313-341.

Nnafie, A., Swart, H.E., Calvete, D., Garnier, R., 2014. Effects of sea level rise on the formation and drowning of shoreface-connected sand ridges, a model study. Continental Shelf Research, 80, 32-48.

Nnafie, A., Swart, H.E., Calvete, D., Garnier, R., 2015. Dynamics of shoreface-connected and inactive sand ridges on a shelf, Part 2: The role of sea level rise and associated changes in shelf geometry. Continental Shelf Research, 104, 63-75.

Olariu, C., Steel, R.J., Dalrymple, R.W., Gingras, M.K., 2012. Tidal dunes versus tidal bars: The sedimentological and architectural characteristics of compound dunes in a tidal seaway, the lower Baronia Sandstone (Lower Eocene), Ager Basin, Spain. Sedimentary Geology, 279, 134-155.

Pérez-Valera, F., Sánchez-Gómez, M., Pérez-López, A., Pérez-Valera, L.A., 2017. An evaporite-bearing accretionary complex in the northern front of the Betic-Rif orogen. Tectonics, 1-31.

Plint, A.G., 1988. Sharp-based shoreface sequences and 'offshore bars' in the Cardium Formation of Alberta: Their relationship to relative changes in sea level. In: Sea-level changes: An integrated approach (Wilgus, Ch. K., Hastings, B.S., Posamentier, H., Van Wagoner, J., Ross, Ch. A., Kendall, Ch. G. St. C., Eds.), SEPM Spec. Pub., 42, 357-370.

Posamentier, H.W., 2002. Ancient shelf ridges—a potentially significant component of the transgressive systems tract: case study from offshore northwest Java. AAPG bulletin, 86, 75-106.

Posamentier, H.W., Chamberlain, C.J., 1993. Sequence-stratigraphic analysis of Viking Formation lowstand beach deposits at Joarcam Field, Alberta, Canada. In: Sequence stratigraphy and facies associations (Posamentier, H.W., Summerhayes, C.P., Haq, B.U., Alllen, G. P., eds.). Spec. Publs .Int. Ass. Sediment., 18, 469-485.

Posamentier, H.W., Morris, W.R., 2000. Aspects of the stratal architecture of forced regressive deposits. In: Hunt, D., Gawthorpe, R.L. (Eds.), Sedimentary Responses to Forced Regressions: Geological Society, London, Spec. Publ., 172, pp. 19–46.

Reolid, M., García-García, F., Tomasovych, A., Soria, J.M., 2012. Thick brachiopod shell concentrations from prodelta and siliciclastic ramp in a Tortonian Atlantic-Mediterranean Strait (Miocene, Guadix Basin, southern Spain). Facies, 58, 549-571

Rodríguez-Tovar, F.J., Pérez-Valera, F., Pérez-López, A., 2007. Ichnological analysis in high-resolution sequence stratigraphy: the Glossifungites ichnofacies in Triassic successions from the Betic Cordillera (southern Spain). Sediment Geol. 198, 293–307.

Roldán, F.J., Lupiani, E., Villalobos, M., Hidalgo, J., Soria, J., Fernández-Gianotti, J. 1994. Mapa geológico de la Hoja nº 971 (Cuevas del Campo). Mapa Geológico de España a escala 1:50.000. Segunda Serie (MAGNA) ©Instituto Geológico y Minero de España (IGME).

Rossi, V.M., Longhitano, S.G., Mellere, D., Dalrymple, R.W., Steel, R.J., Chiarella, D., Olariu, C., 2017. Interplay of tidal and fluvial processes in an early Pleistocene, delta-fed, strait margin (Calabria, Southern Italy). Mar. Petr. Geol., 87, 14-30.

Schwab, W.C., Baldwin, W.E., Hapke, C.J., Lentz, E.E., Gayes, P.T., Denny, J.F., List, J.H., Warner, J.C., 2013. Geologic evidence for onshore sediment transport from the inner continental shelf. J. Coast. Res (29), 526–544.

Sierro, F. J., González-Delgado, J.A., Dabrio, C.J., Flores, J.A., Civis, J., 1996. Late Neogene depositional sequences in the foreland basin of Guadalquivir (SW Spain), in Tertiary Basins of Spain: The Stratigraphic Record of Crustal Kinematics, edited by P. Friend and C. J. Dabrio, pp. 339 – 345, Cambridge Univ. Press, New York.

Snedden, J.W., Bergman, K., 1999. Isolated shallow marine sand bodies: deposits for all interpretations. In: Isolated Shallow Marine Sand Bodies: Sequence stratigraphic analysis and sedimentologic interpretation (Bergman, K.M., Snedden, J.W., Eds.). SEPM Spec. Pub., 64, 1-11.

Snedden, J.W., Dalrymple, R.W., 1999. Modern shelf sand ridges: From historial perspective to a unified hydrohynamic and evolutionary model. In: Isolated Shallow Marine Sand Bodies: Sequence stratigraphic analysis and sedimentologic interpretation (Bergman, K.M., Snedden, J.W., Eds.). SEPM Spec. Pub., 64, 13-28.

Snedden J.W., Tillman, R. W., Culver, A.J., 2011. Genesis and evolution of a mid-shelf, storm-built sand ridge, New Jersey Continental Shelf, USA. Journal of Sedimentary Research, 81, 534-552.

Soria, J.M., 1993. La sedimentación neógena entre Sierra Arana y el río Guadiana Menor. Evolución desde un margen continental hasta una cuenca intramontanosa [Ph.D. Thesis]: University of Granada: Spain, 292 p.

Soria, J.M., Fernández, J., Viseras, C., 1999. Late Miocene stratigraphy and palaeogeographic evolution of the intramontane Guadix Basin (Central Betic Cordillera, Spain): implications for an Atlantic–Mediterranean connection. Palaeogeography, Palaeoclimatology, Palaeoecology, v. 151, p. 255–266.

Soria, J.M., Fernández, J., García, F., Viseras, C., 2003. Correlative lowstand deltaic and shelf systems in the Guadix Basin (Late Miocene, Betic Cordillera, Spain): The stratigraphic record of forced and normal regressions. Journal of Sedimentary Research, 73 (6), 912-925.

Suter, J.R., Clifton, E., 1999. The Shannon sandstone and isolated linear sand bodies: Interpretations and realizations. In: Isolated Shallow Marine Sand Bodies: Sequence stratigraphic analysis and sedimentologic interpretation (Bergman, K.M., Snedden, J.W., Eds.). SEPM Spec. Pub., 64, 321-356.

Schwarz, E., 2012. Sharp-based marine sandstone bodies in the Mulichinco Formation (Lower Cretaceous), Neuquén Basin, Argentina: remnants of transgressive offshore sand ridges. Sedimentology, 59, 1478-1508.

Schwarz, E., Veiga, G.D., Trentini, G.A., Isla, M.F., Spaletti, L.A., 2018. Expanding the spectrum of shallow-marine, mixed carbonate-siliclastic systems: Processes, facies distribution and depositional controls of a siliciclastic-dominated example. Sedimentology, 65, 1558-1589.

Swift, D.J.P., 1978. Tidal sand ridges and shoal-retreat massifs. Marine Geology, 18, 105-134

Trowbridge, J.H., 1995. A mechanism for the formation and maintenance of shore-oblique sand ridges on storm-dominated shelves. J. Geophys, Res. 100 (C16), 16071-16086

van Heteren, S., van der Spek, A., vander Valk, B., 2011. Evidence and implications of middle-to late-Holocene shoreface steepening offshore the western Netherlands. In; Proceedings of the Coastal Sediments, 188-201

Van Wagoner, J.C., 1991. High-frequency sequence stratigraphy and facies architecture of the Sego Sandstone in the Book Cliffs of Western Colorado and Eastern Utah. In: Sequence stratigraphy applcations to shelf sandstone reservoirs. AAPG Spec. Pub., 25, 15-42

Yang, B.C., Dalrymple, R.W., Chun, S.S., 2005. Sedimentation on a wave-dominated, open-coast tidal flat, south-western Korea: summer tidal flat - winter shoreface. Sedimentology, 52, 235-252

Zecchin, M., Catuneanu, O., Caffau, M., 2019. Wave-ravinement surfaces: Classification and key characteristics. Earth-Science Reviews, 188, 210-239

Figures and captions

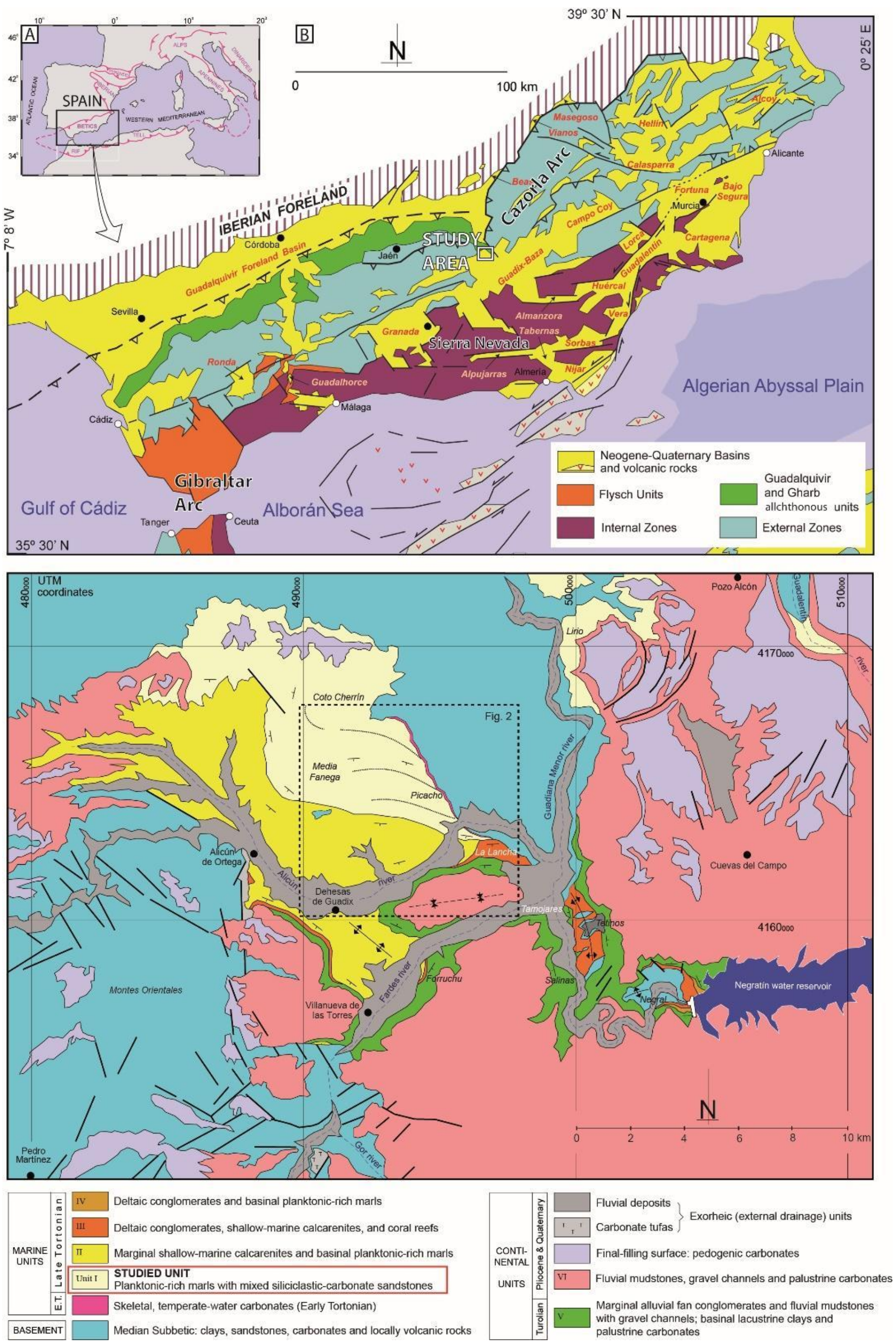

Fig. 1. Location map of the study area within the Iberian Peninsula (A) and in the Betic Cordillera (B), in southern Spain. (C) Geological map (and legend) of the study area, ca. 5 km NE of Alicún de Ortega. Modified from Soria (1993).

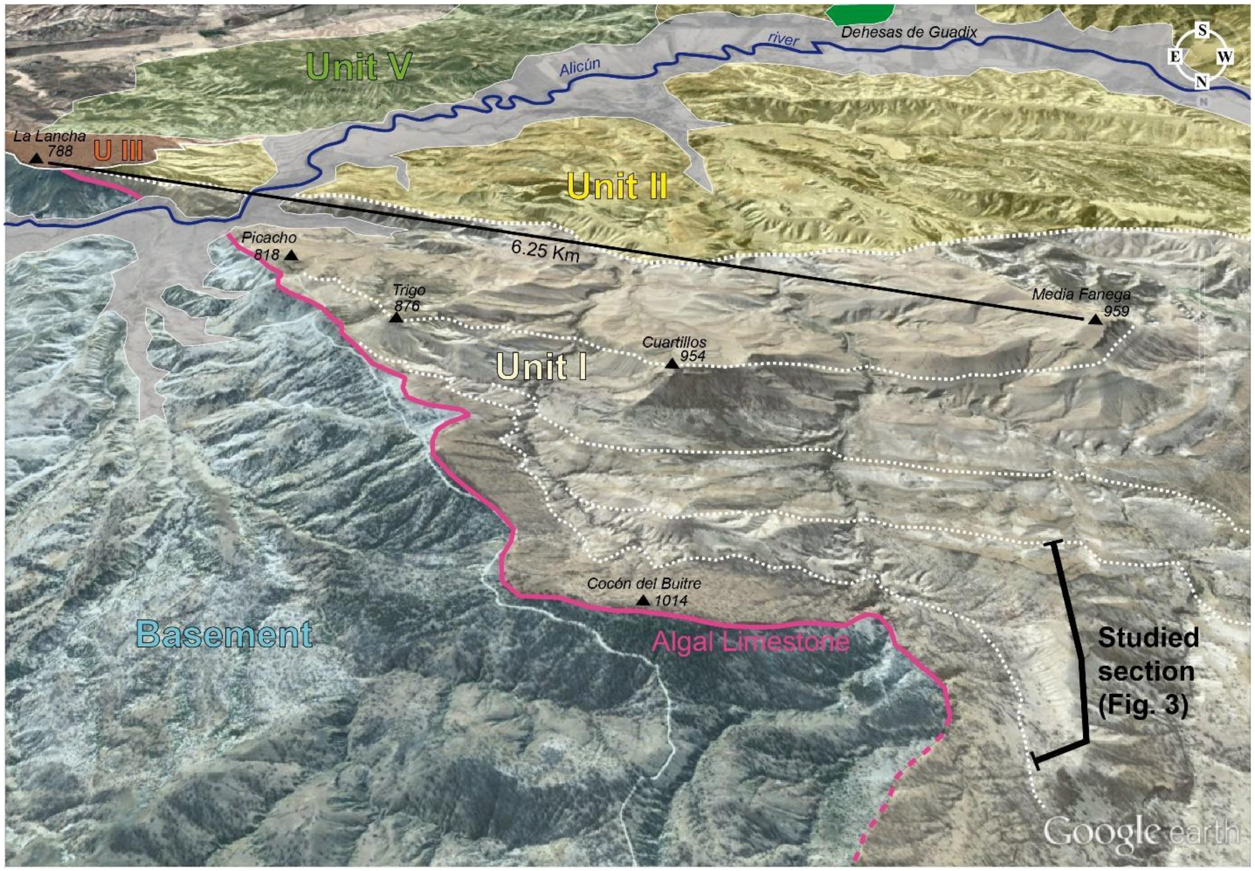

Fig. 2. Interpreted satellite image of the study area, showing the location of the studied section within the upper Tortonian marine (Units I-III) to continental (Unit V) succession (Soria, 1993). See the marked onlap termination of the lowermost marine deposits (Unit I, objective of this study) into a deformed/tilted Serravalian to lower Tortonian Algal unit (Algal Limestone), on top of a basement formed by Mesozoic to Lower Miocene rocks from the External Zone (Pérez-Valera et al., 2017).

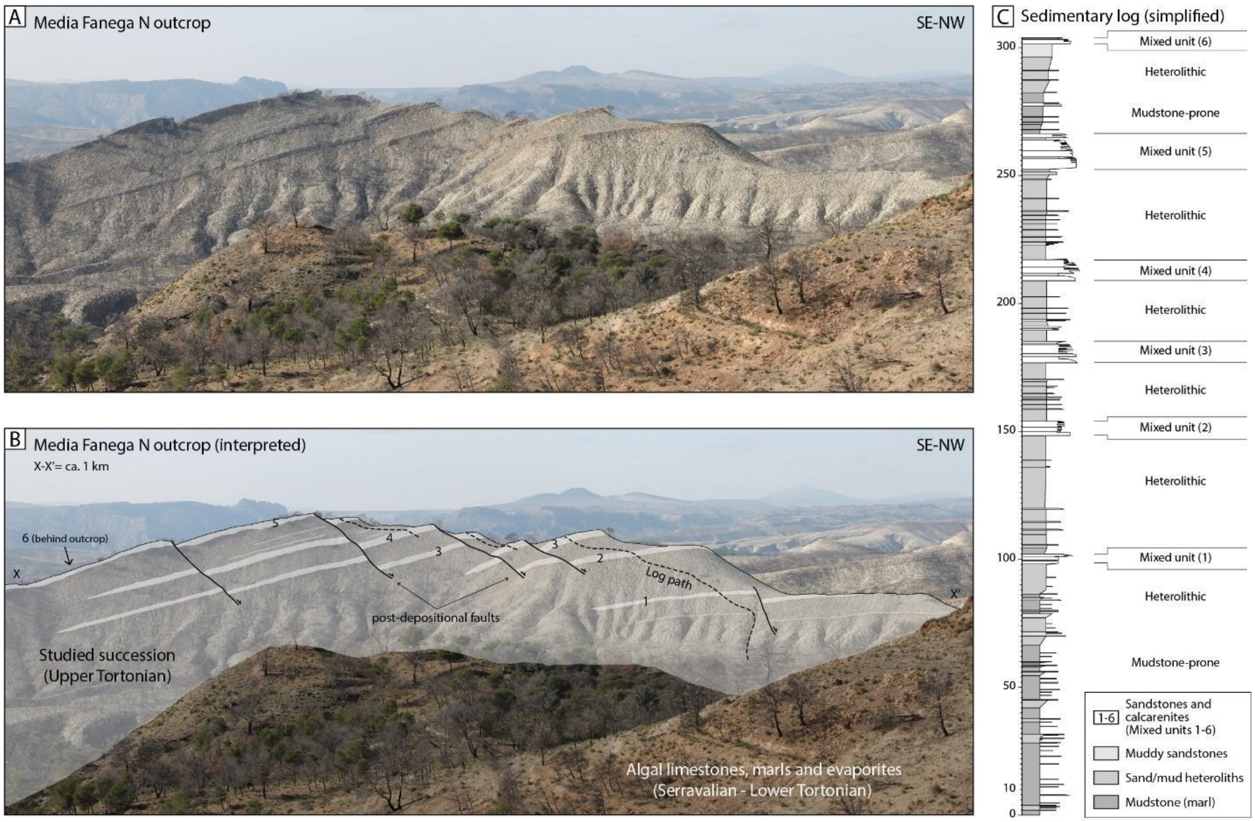

Fig. 3. (A) Uninterpreted and (B) interpreted panoramic view of the Media Fanega North outcrop, the focus of this study. See the alternating succession of upper Tortonian mudstone-prone deposits with several coarser-grained units (1-6), which progressively fine and eventually pinchout or onlap onto the underlying Serravalian to lower Tortonian units towards the SE (see map in Fig. 1). See the intense post-depositional faulting occurred. (C) Simplified sedimentary log of the studied succession, showing the location of several sharp-based, mixed clastic-carbonate units (Mixed units 1-6), within a succession dominated by muddy sandstone and heterlothic deposits.

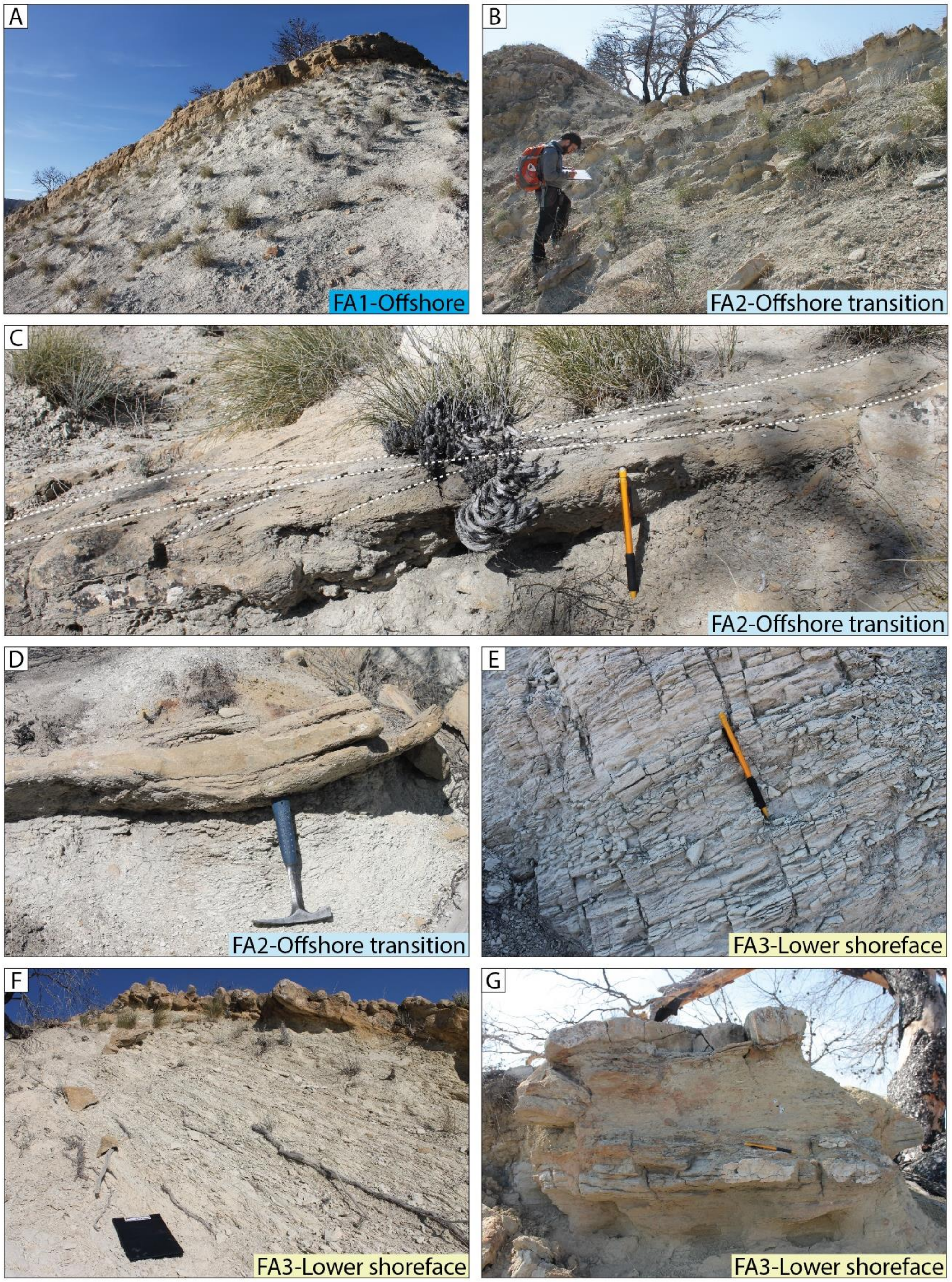

Fig. 4. Field photos of the different facies recognized in the study area. (A) Thick (several m-thick), light grey structureless or faintly laminated mudstones (offshore, FA1), which dominate the lower part of the succession. (B) Alternating sand/mud heterolithic packages with cm-thick muddy sandstones (offshore transition, FA2). (C) Example of hummocky-cross stratified sandstone, particularly common in the lower part of the succession (offshore transition, FA2). (D) Example of recurrent soft-sediment deformation in hummocky-cross stratified sandstone (offshore transition, FA2). (E) Ripple cross-laminated muddy sandstones (lower shoreface, FA3). (F) Coarsening-up heterolithic to muddy sandstone package (lower shoreface, FA3). (G) Low angle cross-stratified muddy sandstones (lower shoreface, FA3).

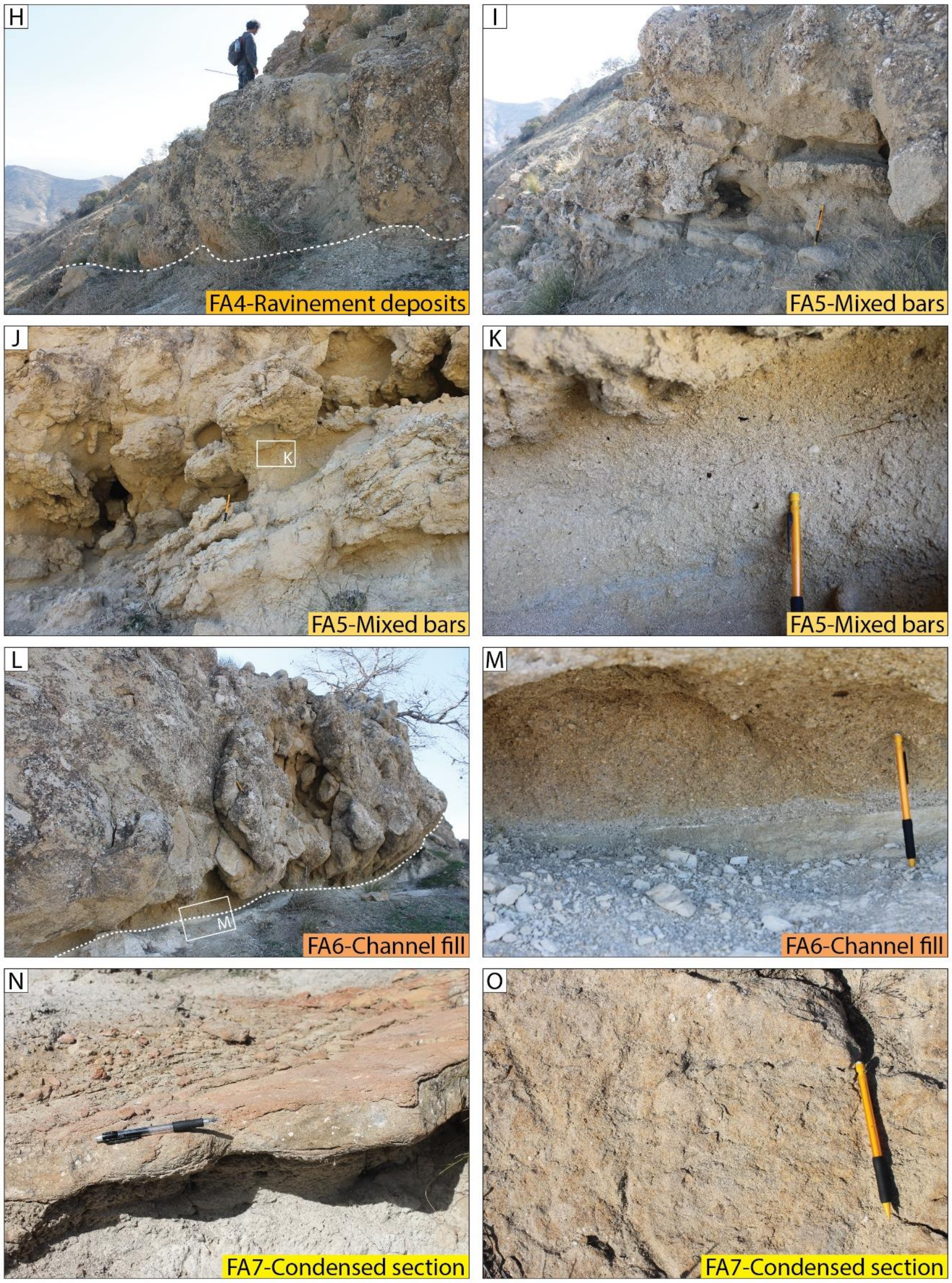

Fig. 4 (continued). Field photos of the different facies recognized in the study area. (H) Sharp-based, bioclastic mixed carbonate-clastic bed (ravinement deposits, FA4); see the abrupt (and commonly bioturbated) nature of the base of these deposits. (I) Large-scale cross-stratified mixed clastic-carbonate deposits (mixed bars, FA5). (J) Highly bioturbated, cross-stratified mixed clastic-carbonate deposits (mixed bars, FA5). (K) Inset view of (J) showing the coarse-grained and highly bioclastic nature of mixed bar deposits (FA5), with intrabasinal skeletal fragments, extraclasts, and coal. (L) Erosive-based, channelized bioclastic medium to coarse grained sandstone deposits (channel-fill, FA6). (M) inset view of (L) showing the major grain size break across the erosive base of channel-fill deposits (FA6), cutting into lower shoreface muddy sandstones (FA3). (N) Oxidized, thin-bedded, bioclastic and glauconitic sandstone (condensed deposits, FA-5). (O) Detail view of the top surface of a highly bioturbated, bioclastic and glauconitic sandstone (condensed deposits, FA-5).

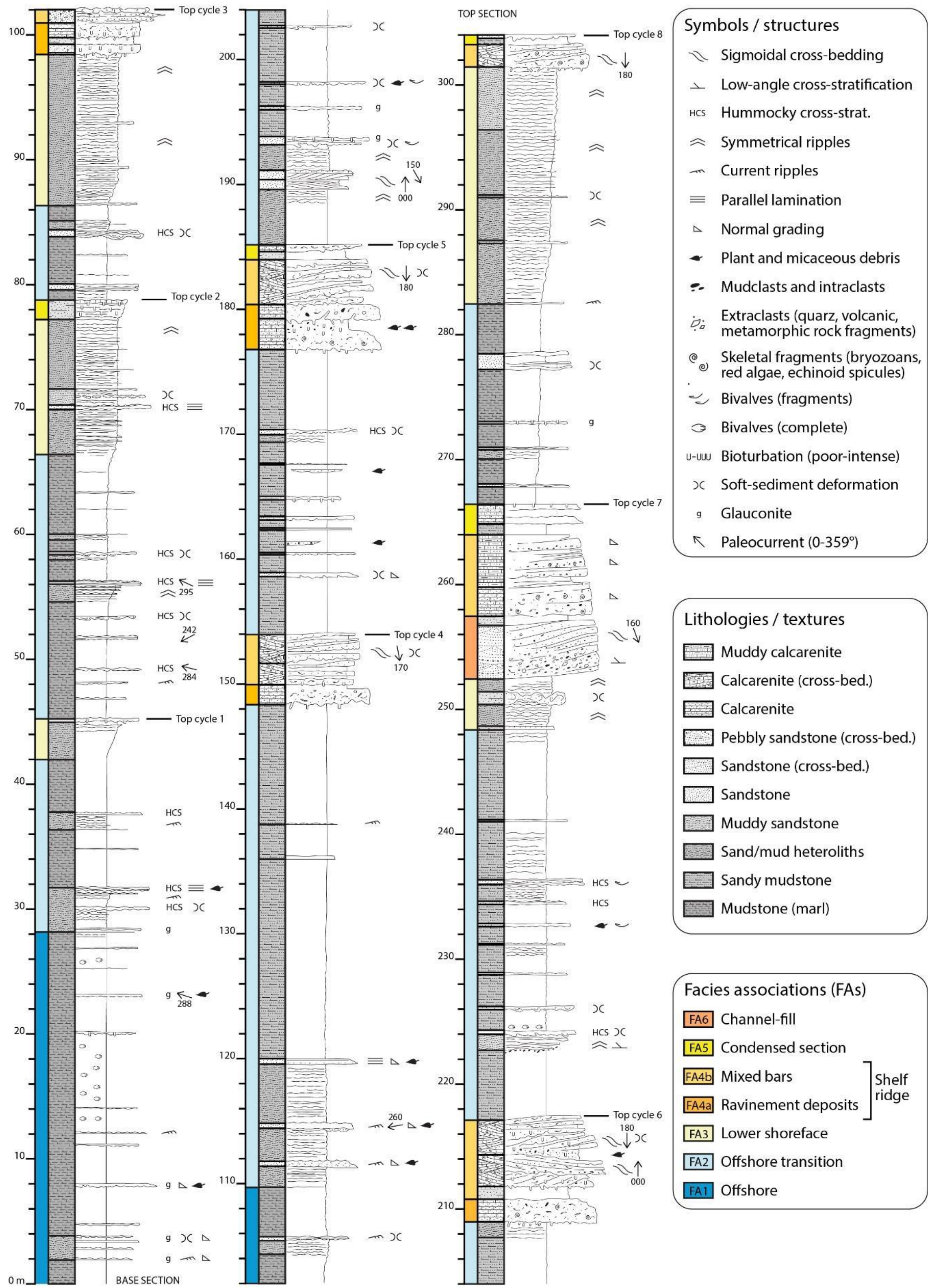

Fig. 5. Detailed sedimentary log of the studied succession (see location in Fig. 3).

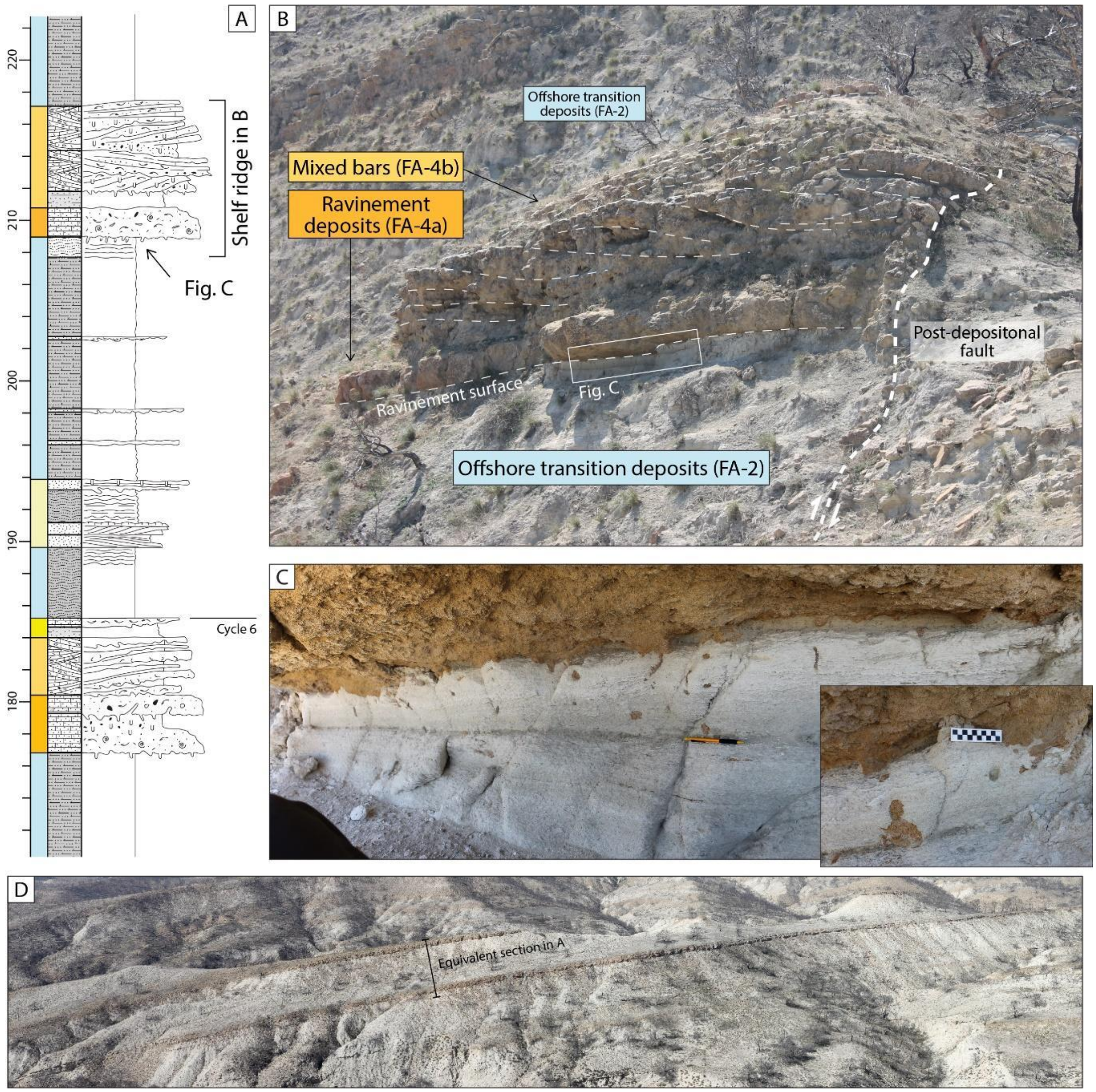

Fig. 6. Example of the mixed clastic-carbonate units analysed in this study. (A) Fragment of the studied section showing the common stratigraphic arrangement of mixed units, abruptly truncating offshore transition (sometimes also lower shoreface) deposits. (B) Field example of one of these units, highlighting the sharp nature of the basal, highly bioturbated contact, interpreted as a ravinement surface. The surface is often overlain by a skeletal-rich bioclastic calcarenite (FA4), and by large-scale sigmoidal cross-bedded calcarenites, forming accreting barforms (FA5). These deposits combined are interpreted as mixed carbonate-clastic shelf ridges. (C) Outcrop photo highlighting the sharp-based, sharp-topped nature of the mixed clastic-carbonate units, as well as their lateral extension (100s of m). These units tend to show a more amalgamated nature in the central, axial part, and progressively thin and interfinger with the underlying and overlying offshore transition deposits.

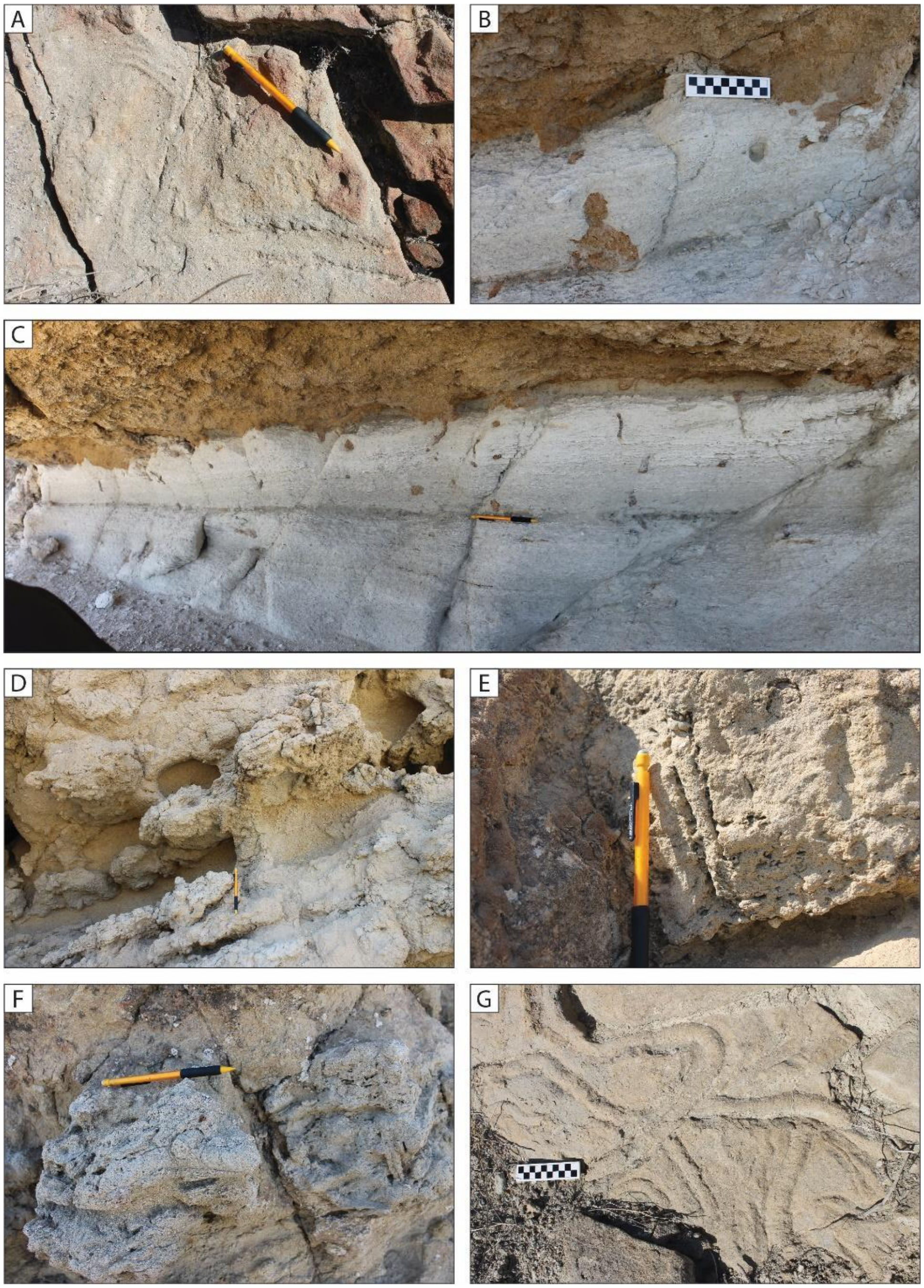

Fig. 7 – Examples of trace fossils found in the studied section. A) Horizontal *Ophiomorpha* at the upper surface of a storm bed, showing T-shaped branching and pellets along the wall (offshore transition FA2). B-C) Vertical, and oblique burrows, as well as circular sections, passively infilled by mixed carbonate-clastic sediments (ravinement deposits, FA4), located into the light sandy siltstone deposits below (lower shoreface, FA3). D) Frequent bioturbation in mixed carbonate-clastic cross beds (mixed bars, FA5), with dominant *Planolites* and well-developed *Thalassinoides* structures. E) Vertical shaft of probable *Ophiomorpha* (pellets along the wall can be envisaged) (mixed bars, FA5). F) *Bichordites*/*Scolicia* traces showing cross-cutting relationships and similar infilling material than the host mixed carbonate-clastic sediment (mixed bars, FA5). G) Several traces of *Scolicia* showing cross-cutting relationships in the upper surface of a bioclastic sandstone bed (condensed section, FA6).

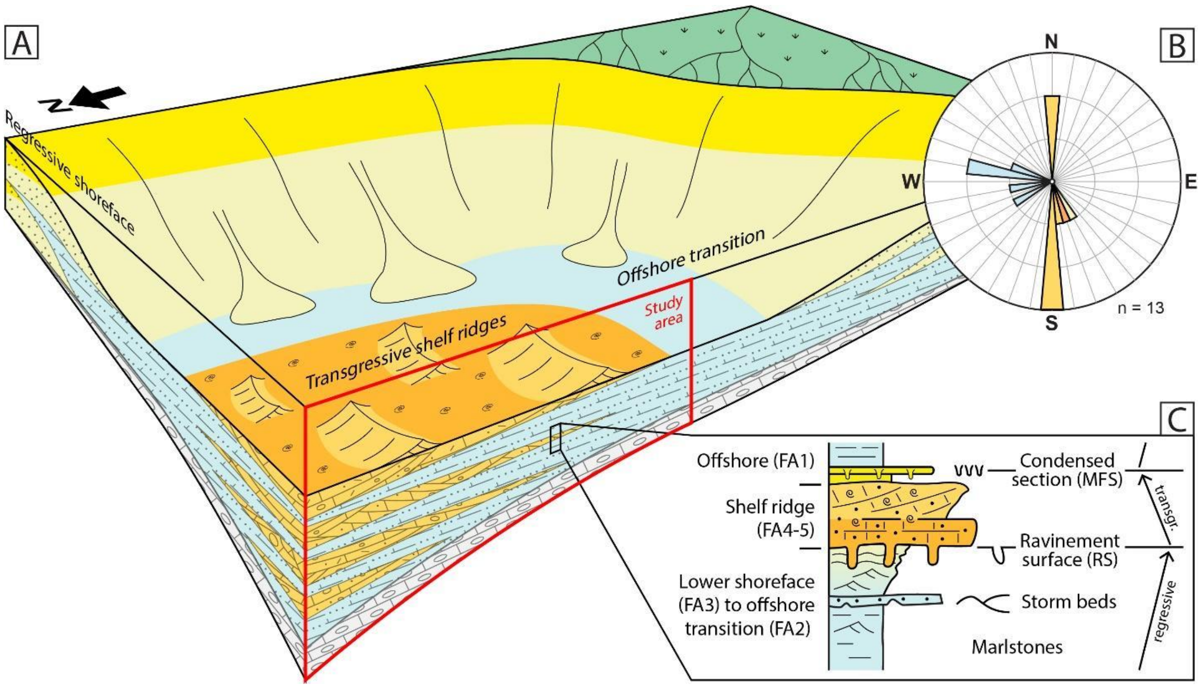

Fig. 8. (A) Depositional model, (B) Paleocurrent distribution (coloured according to the FA codes) and (C) idealized cycle of the mixed carbonate-clastic shelf ridges for the studied succession. The common cyclic arrangement shows offshore mudstones (FA1), progressively replaced by offshore transition deposits (FA2), with sandy mudstones interbedded with sandstone beds with combined-flow structures and soft-sediment deformation. In some cases, the cycles preserve a vertical transition from offshore transition to lower shoreface muddy sandstone deposits (FA3), with wavy bedding and symmetrical ripples, in an overall regressive trend. However, these regressive successions are abruptly truncated by a sharp, highly bioturbated contact, interpreted as a transgressive ravinement surface (TRS). Above this, skeletal-rich bioclastic calcarenites (FA4) and large-scale sigmoidal cross-bedded calcarenites (FA5), forming mixed carbonate-clastic shelf ridges, commonly stack in common fining, thinning-up trend, consistent with their transgressive character. The cycles often culminate in either a sharp top or in a thin, highly bioturbated package (FA7), interpreted as a condensed section containing a maximum flooding surface (MFS). This surface marks the boundary between cycles, as it is often overlain by offshore (FA1) or offshore transition deposits (FA2) of the overlying cycle.

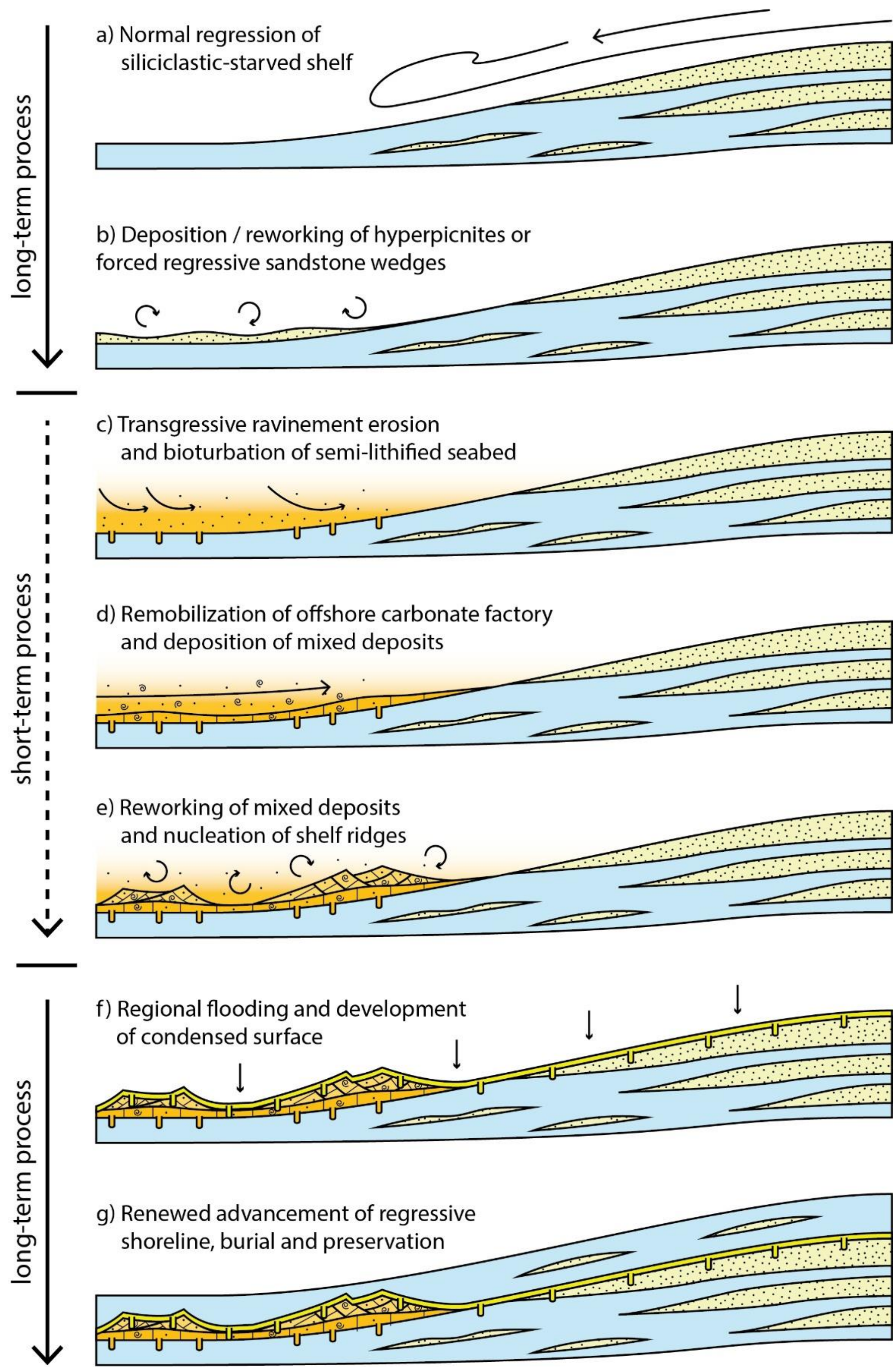

Fig. 9. Proposed evolutionary model for the development and preservation of sharp-based, mixed carbonate-clastic shallow-marine deposits, interpreted as transgressive shelf ridges. See text for a more detailed description of the different stages (A-F).